AFDELINGEN FOR MATERIALEFORSKNING

MICROSTRUCTURAL PROPERTIES AND FATIGUE BEHAVIOUR OF HIGH STRENGTH TOOL STEELS.

POVL BRØNDSTED

✉: Postboks 49,
4000 Roskilde,
☎: 4677 5704,
💻: povl.brondsted@risoe.dk

Abstract

More than 80% of tools in cold forging fail because of fatigue damage due to cyclic loading. In the present paper methods developed to describe the relationship between microstructure and mechanical properties of tool steel materials are presented. Carbide types and carbide size distributions have been identified. Microstructural features such as carbides and their sizes and size distributions appear to be important controlling factors in the degradation of the material. The damage evolution has been studied and sources for crack initiation were identified.

Phenomenological models can be used to estimate the lifetime. Here is presented a model based on calculating the energy dissipated in the material during cyclic loading. Using this model, lifetime predicition can be made and lifetime curves can be established based on short time fatigue tests. In examples it is shown how lifetime curved can be presented in a 3-D space, and the relations between fatigue parameters are visualised.

Introduction

High strength tool steels (classified according to the AISI system as high-speed steels) are complex iron-base alloys with strong carbide forming elements such as Cr, V, W and Mo, and they may contain more than 30 vol.-% carbides embedded in a martensitic matrix[1,2]. The steels are applied in forging- and cutting tools and are in these applications exposed to alternating mechanical loads and/or changing thermal conditions. Consequently, fatigue damage is usually what limits the life of the tools and fractured carbides apparently play an important role in the damage process of crack initiation and propagation [3]. The carbides are subject to very high residual stresses, which result from the differences in thermal expansion and Young's moduli between the matrix and carbides [4].

More than 80% of tools in cold forging fail because of fatigue damage due to cyclic loading. In a European frame programme "Improvement of Service Life and Reliability of Cold Forging Tools with respect to Fatigue Damage due to Cyclic Plasticity" (COLT) methods have been developed to describe the relationship between microstructure and mechanical properties of tool steel materials.

Phenomenological models can be used to estimate the lifetime. One model is based on calculating the energy dissipated in the material during cyclic loading. Other models describing tool loadings has been suggested and are used in the COLT project [5,6,7,8,9,10]. It has been shown that it is possible to describe the tool loads and hence make demands on the material performance. In order to make the optimal material selection it is of the greatest importance for the sensitivity of the models to be able to define and to measure the strength-controlling material parameters as accurate as possible. Thus it will often be the limitations of the material, which control the tool design and the material limits the application. It is the

close correlation between design wishes and the possible obtainable material properties, which is the core in this optimisation process.

To optimise the performance of a tool steel it is therefore important to consider the microstructure and particularly the sizes, types and distribution of carbides. Also, non-metallic inclusions are expected in the steels and it is important to quantify their sizes and distributions in order to evaluate the influence of their presence.

Materials

Typical high strength steel materials are P/M (powder metallurgical) high-speed tool steels like for example the classic Vanadis 23 delivered by Uddeholm Tooling AB, Sweden, and the S390 delivered by Böhler. Compositions of these two steels are given in Table 1.

Table 1. Composition of PM tool steels.

Steel grade	C	Cr	Mo	V	W	Co
Böhler S390	1.64	4.8	2	4.8	10.5	8
Uddeholm Vanadis 23	1.28	4.2	5.0	3.1	6.4	

Heat Treatment and Microstructures

The microstructure of high-speed tool steels consists of tempered martensite containing finely dispersed carbides. Normally the steels are delivered in fully annealed condition and a three-step heat treatment is applied. Each step introduces new changes to the microstructure and has influence on the final properties of the tool steel. The three steps are: Austenitizing, quenching and tempering.

The general procedure for the heat treatment of tool steels is shown in Figure 1.

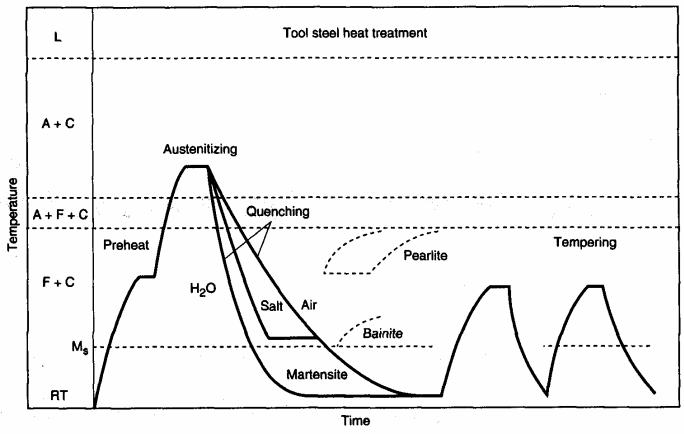

Figure 1. Schematic diagram of tool steel heat treatment steps for final hardening [4].

Austenitizing is done in the austenite and carbon area of the phase diagram. The process temperature and holding time is chosen to obtain a homogeneous microstructure and simultaneously avoiding excessive grain-growth. The chosen austenitizing temperature is decisive for the amount of undissolved carbides (primary carbides) and the amount of carbon and alloying elements in the austenite phase, whereby final carbon volume fraction, hardenability, retained austenite content, and secondary hardening potential are all influenced.

The quenching is a diffusionless transformation of austenite into martensite. The cooling rate must be high enough to ensure that the diffusion of carbon and other alloying elements are avoided but not so high that dimensional changes or heat cracks are introduced.

The final step, tempering, is performed in order to increase the toughness and fracture resistance of the tool steel. The martensite present in the quenched condition is too brittle to be of use in tool application. The tempering takes place in the ferrite and carbon area of the phase diagram (~500-600˚C) and often two or three tempering steps of duration of approximately one hour each are applied. During the tempering the highly alloyed tool steels also experience secondary hardening due to the precipitation of minute secondary carbides coherent with the matrix.

The steels produced by the P/M technique provides a much more homogeneous structure and a much finer dispersion of the carbides. This is especially important when the material is to be used as a tool for cold forging, since the coarse carbides in the wrought steel can act as crack initiation sites.

Figure 2 shows optical micrographs of the microstructure of traditional P/M steels. The small and finely dispersed carbides of the P/M structure improves the resistance against fracture and thereby fatigue cracking[11], and also makes it possible to use higher alloy contents compared to the conventional wrought materials. Due to the small sizes of the carbides Scanning Electron Microscope (SEM) is often used in characterizing the structure. Figure 3 shows SEM backscattered electrons (BSE) micrographs showing the distribution of carbides.

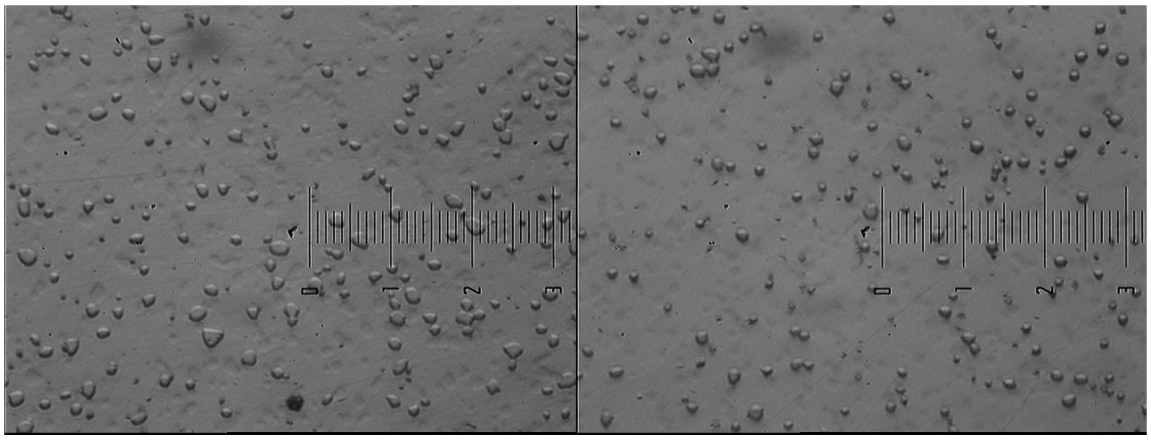

Figure 2. Two Light Optical Microscopy pictures of traditional P/M steel taken with 1010x magnification, one division on the scale equals 1 μm.[12]

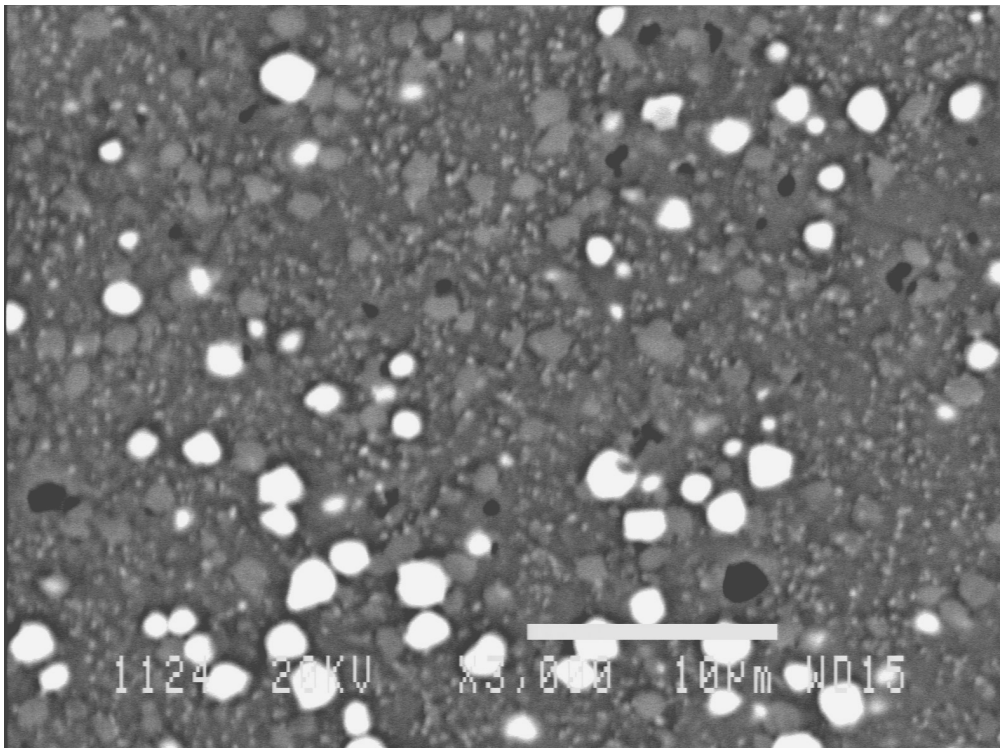

Figure 3. SEM micrograph (BSE contrast) of as delivered Vanadis 23 etched in 5 % nital. The relatively large primary carbides appear in two shades of grey. The light grey (white) primary carbides are identified as M_6C type. The darker grey primary carbides are smaller in size and are identified as V_8C_7 type. The dispersed small secondary carbides are mainly of $M_{23}C_6$ type (the black "particles" are holes left by carbides, which have fallen out during sample preparation).

The size distribution of the carbides can be quantified using quantitative image analysis of the BSE images. Two types of carbides were identified: an M_6C type (M=Fe, W, Mo) and a V_8C_7 type [13]. QIA was performed using the software Image Pro Plus. An example of size distributions of Vanadium carbides in S390 are shown in Figure 4 and size distribution for $(MO,W)_6C$-carbides are shown in Figure 5.

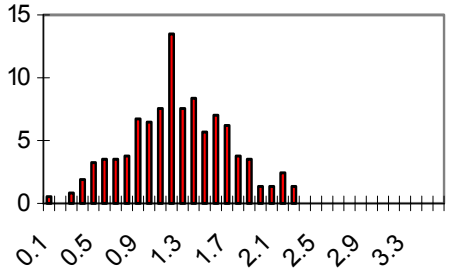

Figure 4. Vanadium carbide size histograms based on EDS-maps

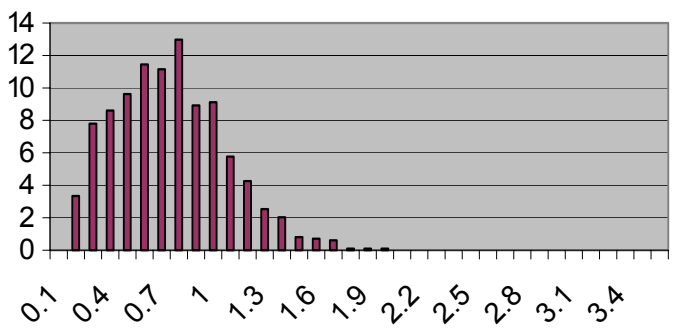

Figure 5. Size distribution for $(Mo,W)_6C$-carbides; x-axis: mean diameter in μm; y-axis frequency in percentage.

Also non-metallic inclusion can be found. Such inclusions can be very damaging. A BSE image of a hole from an inclusion is seen in Figure 6. The non-metallic inclusion is expected to have fallen out during the grinding preparation of the specimen.

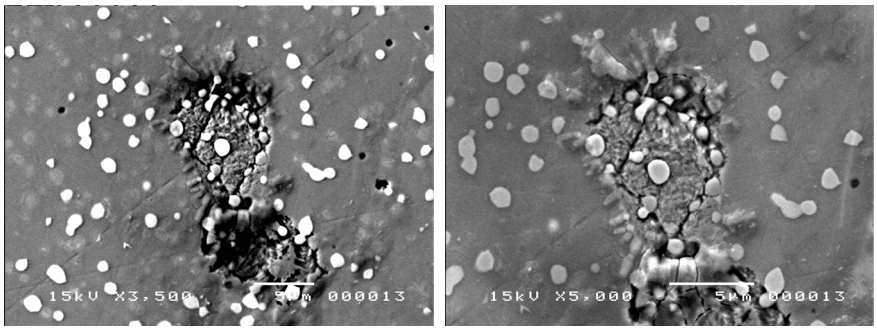

Figure 6. BSE image (left) and SE image (right) of hole from non-metallic inclusion

Fatigue Properties

Uniaxial fatigue testing was carried out under controlled strain conditions with constant strain amplitudes [14].

The specimen geometry used in the mechanical tests was optimised from an earlier geometry shown in Figure 7 and the optimisation procedure is shown in Figure 8. The optimisation was carried out by STRECON®.

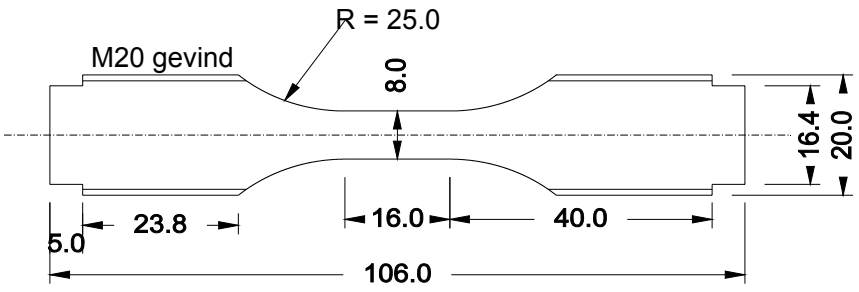

Figure 7. First geometry of universal test specimen.

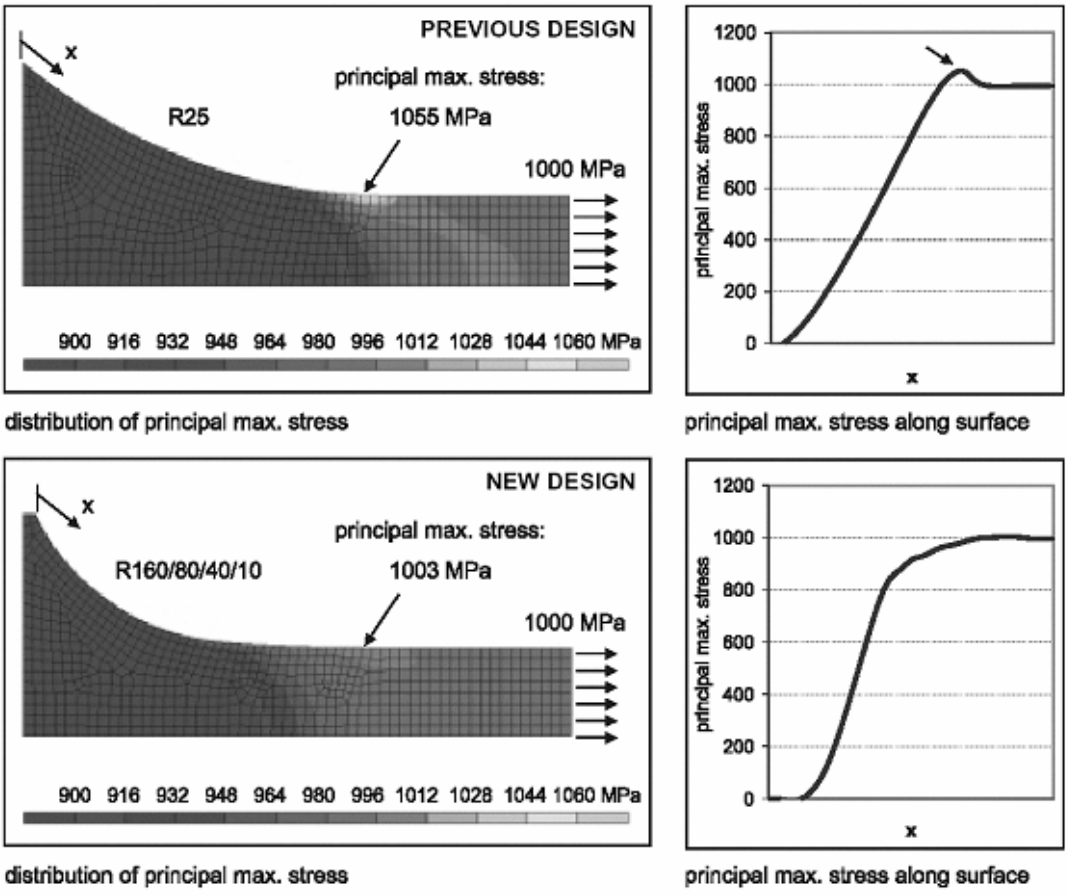

Figure 8. Optimisation of test specimen geometry. (Courtesy of STRECON® A/S)

The combined tension-compression testing requires column stability of the test specimen so that buckling is avoided under the compressive load. This requires in addition to a relatively short gauge length an extremely rigid mounting. This has shown to be possible by using a servo hydraulic combined tension/compression/torsion universal test machine, as the hydraulic cylinder in this equipment has additional bearings due to the torsion facilities. Strain has been monitored using a laser extensometer as shown in the set-up in Figure 9. The load is measured using a ±250 kN load cell.

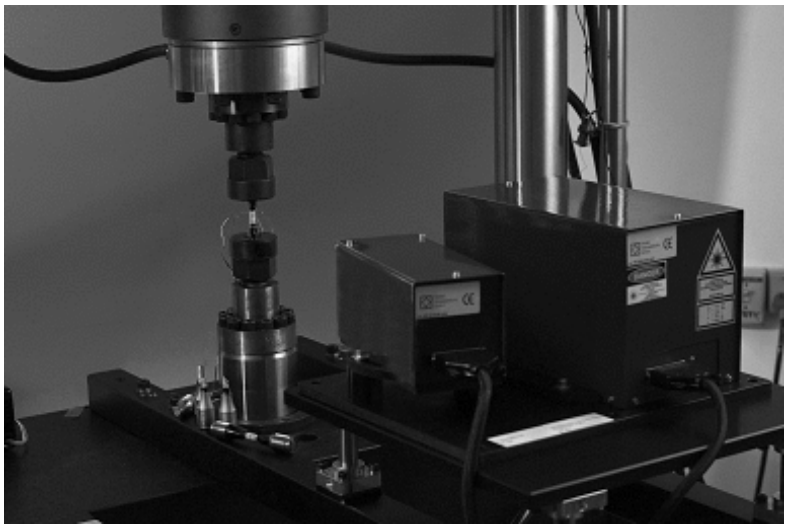

Figure 9. Set-up for tension/compression testing using laser extensometer.

Test Programme and Data Analysis

An extensive test programme was carried through. Steels were tested to failure under constant R-ratios (constant $\varepsilon_{max}/\varepsilon_{min}$ ratios), under constant mean strain values and in step tests. All tests were low cycle fatigue tests running less than 30,000 cycles at 0.25 Hz. The test results were analyses according to the following.

A strain-controlled test is characterised by two independent loading parameters. It can be two of the following:

- Maximum strain: ε_{max}
- Minimum strain: ε_{min}
- Fatigue ratio: $R = \varepsilon_{min}/\varepsilon_{max}$
- Strain Amplitude: ε_{ampl} or strain range $\varepsilon_{range} = 2 \cdot \varepsilon_{ampl} = (\varepsilon_{max} - \varepsilon_{min})$
- Mean Strain: $\varepsilon_{mean} = (\varepsilon_{max} - \varepsilon_{min})/2$

The tests results in the dependent parameter

- Number of cycles, N

The resulting stress values are measured functions of the number of cycles:

- Maximum stress: σ_{max}
- Minimum stress: σ_{min}
- Stress Amplitude: σ_{ampl} or stress range $\sigma_{range} = 2 \cdot \sigma_{ampl}$
- Mean Stress: σ_{min}

Based on these measurements the cyclic saturation stresses ($\sigma_{sat,\,max}$,$\sigma_{sat,min}$) are defined as the peak stress levels where σ_{max} and σ_{min} becomes independent of N, and hence a cyclic stress strain curve can be defined.

During a test all stress strain loop data are sampled. Each loop consists of at least 100 data points. Each loop was integrated in order to calculate the amount of energy dissipated in the loop. The average loop area for each test is calculated. For each loop the maximum and the minimum values of stress and strain are found. This means that the following data from the test are available:

N_f: Number of cycles to failure

N_i: loop number

ΔA_i: Hysteresis area of loop number "N_i"

ΔA_{avg}: The average area of all hysteresis loops in the saturation sequence (i.e. where σ_{max} and σ_{min} are constant)

A_{total}: Accumulated loop area

$(\sigma,\varepsilon)_i$: datapoints for loop "N_i"

$(\sigma_{max},\varepsilon_{max})_i$: highest vaules for loop "N_i"

$(\sigma_{min},\varepsilon_{min})_i$: lowest vaules for loop "N_i"

An example of data from a test series is shown in Table 2.

The data are analysed in the following way:

A relation between average hysteresis loop area ΔA_{avg} and number of cycles to failure (N_f) is suggested. It has been found that the following relation between these variables is descriptive:

$$N_f = Const \cdot \Delta A_{avg}^{\ n} \qquad (1)$$

An example on such a relation is shown in Figure 10

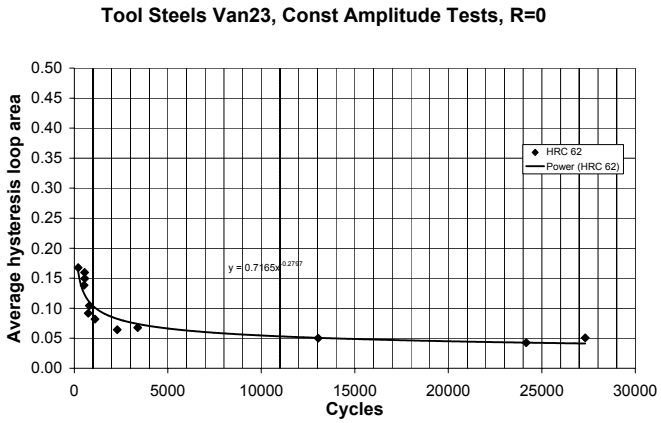

Figure 10. Relation between ΔA and N_f

The relations between the strain range and the number of cycles to failure at a constant R level is shown in Figure 11. This is a traditional Wöhler or S-N curve. The relation between strain range and number of cycles to failure can be described by the well-known Basquin equation:

$$N_f = Const \cdot \Delta\varepsilon^m \qquad (2)$$

During a fatigue test where ε_{range} is constant the hysteresis loop area is measured. If the relation (1) between N_f and the area is known for the specific R-value or a constant mean strain value, the resulting N_f, can be estimated only by running the test into the saturated sequence. This means that a fatigue test should not necessarily be run to the failure of the specimen. If it can be assumed that the resulting hysteresis loops are independent of the prehistory the high cycle fatigue life time can be found from step tests, where the steps are run at constant R or constant mean conditions and only into the saturated sequences.

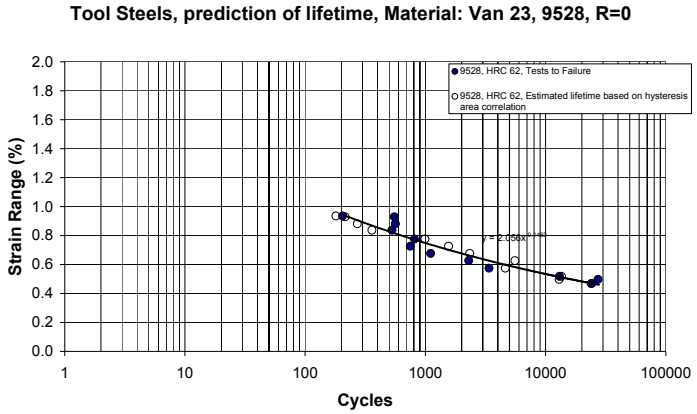

Figure 11. S-N curve for constant R-value

3D Presentation of Fatigue Data

The Wöhler diagram (or SN-curve) describes the relation between the loading amplitude parameter (in this case the strain range) and the number of cycles to failure with a constant mean value or R-value. See Figure 12.

The third dimension in the fatigue parameter space is illustrated in the so-called Haigh diagrams. A Haigh diagrams is shown in Figure 13. Here the relation between ε_{mean} and ε_{range} is shown. A point in this type of diagram represents a given number of cycles to failure, e.g. one point is marking at which range and mean level the lifetime will be 10,000 cycles. The

lines shown in the figure shows “iso-R” lines and test results from tests run at constant R-values lie on these lines. If the test results are positioned on vertical lines it means that the test were run at constant mean values.

Different models have been suggested to describe the results plotted in so-called Haigh or Goodman diagrams. Until now no model has been found to describe the present material behaviour. However, the most uncomplicated model is Goodman lines which shows the limitation in the diagram as straight lines. If it for a tool steel is assumed that the maximum static strain value is 1% and the minimum static compression strain is –3% the limitation lines (corresponding to static tests, or cyclic tests with one cycle) will be as illustrated in Figure 13.

Combining the Haigh diagram and the Wöhler diagram gives a three-dimensional plotting of the fatigue results. This is shown in Figure 14.

In these illustrations it is seen that Wöhler diagrams are the planes that all holds the X-axis and the point (0,0,0) and the normal of these planes rotates 0 to 360 degrees in the y-z plane. This is contrary to the SN curves for constant ε_{mean}, which are all the x-z planes at different constant y values.

If then the Goodman model and the Basquin model can be assumed the limiting lifetime planes in the three-dimensional graphing will be logarithmic envelope planes. However, to verify this a huge amount of data is required and this has not been achieved yet.

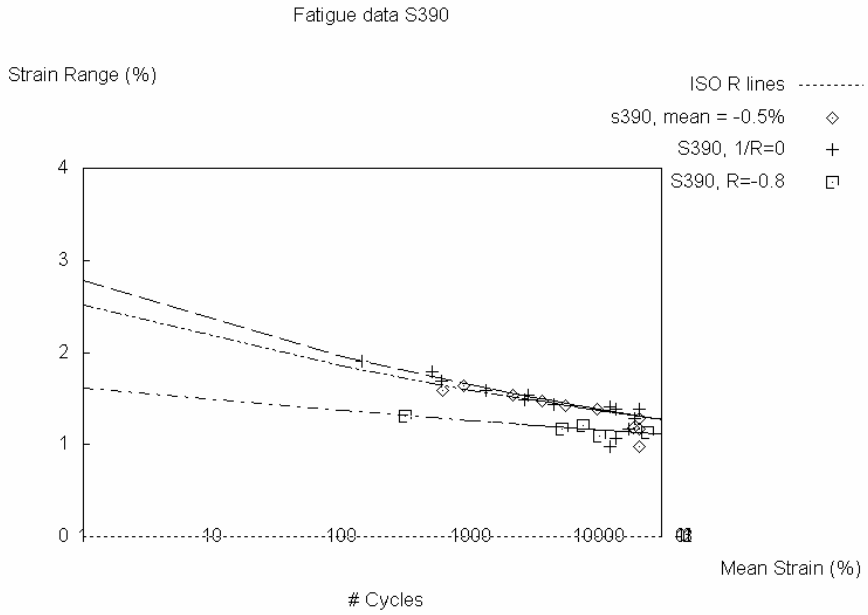

Figure 12. Wöhler - SN diagram, showing the relation between Strain Range and Number of Cycles to failure

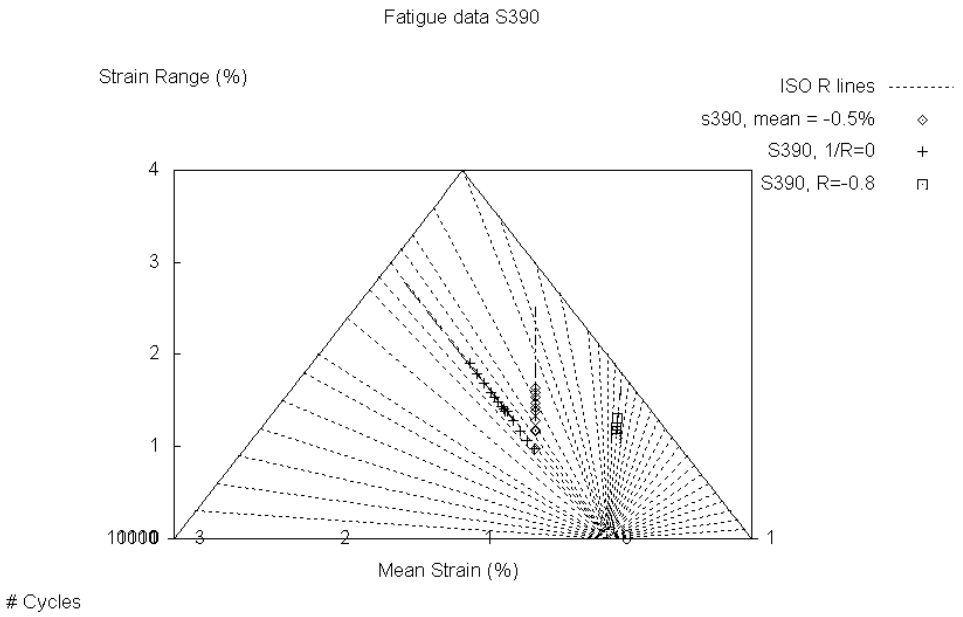

Figure 13. Haigh diagram showing relation between strain range and mean strain.. The lines shown are constant (iso-) R lines. The three tests plotted are two tests run under constant R-values and one test run under constant mean strain.

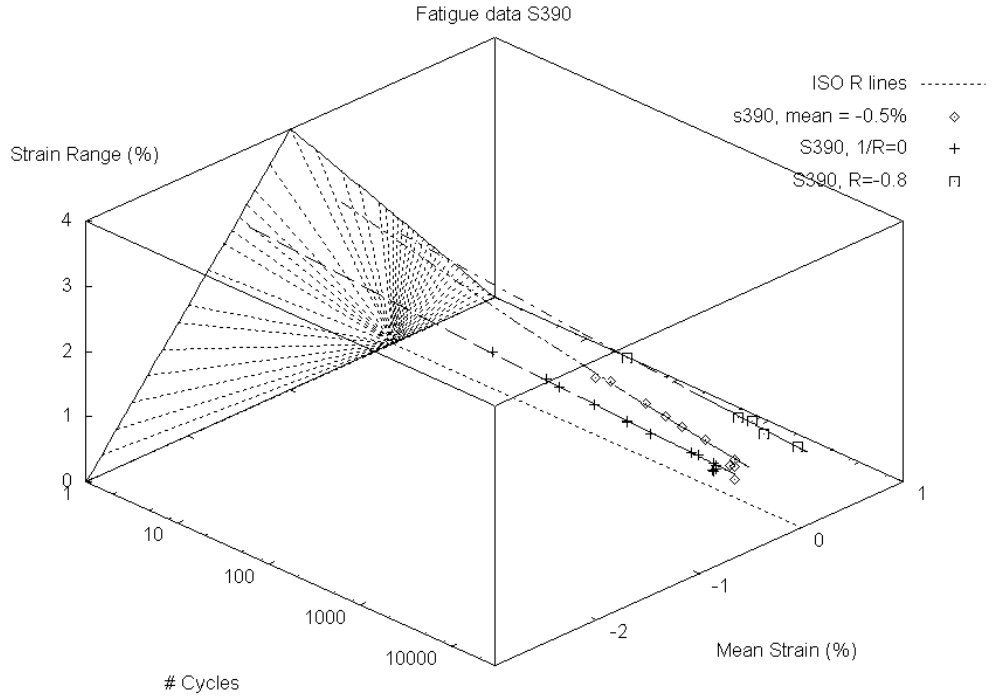

Figure 14. 3D plot of fatigue data. The lines and points corresponds to the data shown in Figure 12 and Figure 13.

Fatigue Damage in the Microstructure.

Both carbide types were found to fracture immediately when exposed to a stress exceeding a threshold value of maximum 80 % of the yield strength. Apparently it was impossible to initiate fatigue crack growth at applied loads too low to cause carbide damage. Thus, it is suggested that crack initiation requires the presence of fractured carbides. It has been found that cracked carbides can be the initiation point of micro cracks. Several cracked carbides have been observed in the area near the bottom of a crack as can be seen from Figure 15. Test specimens subjected to loading conditions are investigated in order to quantify the cracked carbides and inclusions, which can be the initiation points for fatigue damage. Carbide fracture depends on the size as well as the type of carbide. The critical diameter was found to be approximately 0.8 and 1.2 µm for V_8C_7 and M_6C, respectively. The fractured carbides act as crack initiators, probably by causing local cyclic plastic deformation in the matrix, which eventually results in the formation of micro cracks in the matrix.

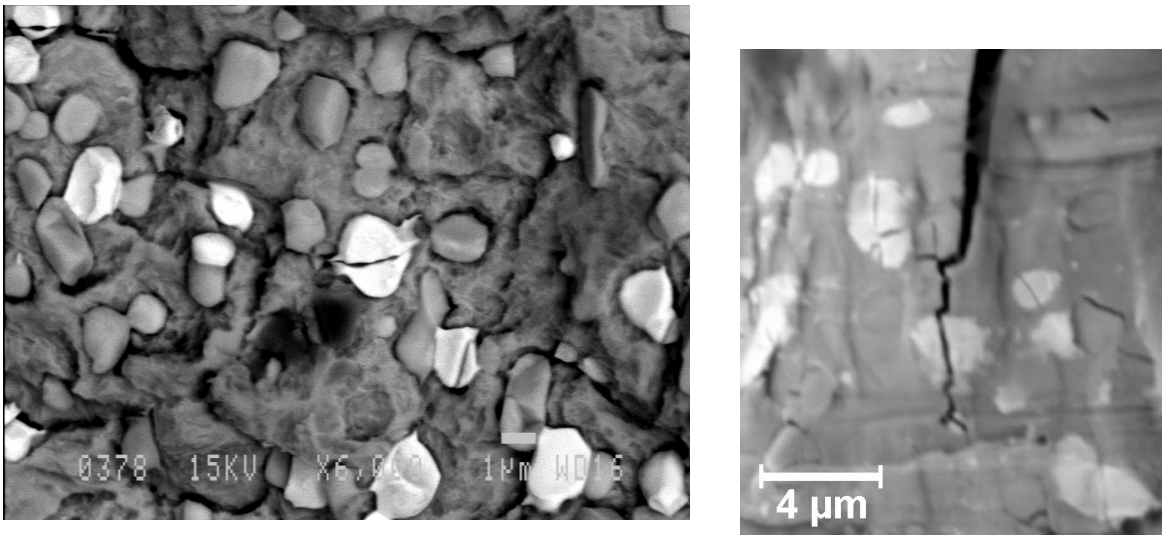

Figure 15. SEM-BE pictures of cracked carbide and fatigue crack.s.

Summary

In this article I have described techniques used to identify the microstructure in tool steel and techniques to quantify microstructural features, which can be sources for fatigue damage initiation. New models to predict fatigue lifetime based on plastic deformation work have been presented for the first time. Also a three-dimensional fatigue result analysis has been shown, and it has been demonstrated that it is evident that cracked carbides plays a considerable role in crack initiation and growth. At this state of the project it has not been possible to release more detailed data and results because that the data handling are still not finished and due to confidentiality between project partners.

Acknowledgements and Concluding Remarks.

The work presented in this article is a part of a European frame programme "Improvement of Service Life and Reliability of Cold Forging Tools with respect to Fatigue Damage due to Cyclic Plasticity".

The consortium consists of seven partners from six European countries. It comprises Krupp Presta (LI) who is a producer of cold forging components, STRECON® (DK) manufacturer of tooling systems, Böhler Edelstahl (AT) supplier of tool steel material, Rockfield Software (UK) and C3M (SI) who are specialised in the development of finite element systems and optimisation software. LFT from University of Erlangen-Nuremberg which is a high education institute active in the areas of material forming, tribology, surface treatment and statistical lifetime predictions. Risø National Laboratory (DK) has contributed with advanced material testing, modelling and microstructural investigations.

In connection with the COLT project a PhD. project by Christian Højerslev was successfully accomplished[15]. The PhD. project was carried out in The Engineering Science Centre for Structural Characterisation and Modelling of Materials (IVC) at Materials Research Department, Risø National Laboratory. The financial support from both the EU 5th frame programme and the Danish IVC are gratefully acknowledged.

Finally I will like to express my thanks to all persons involved in the project. Especially the collaboration and able assistance from Senior Scientist Jesper V. Carstensen, PhD student Christian Højerslev, student assistants Kristian Vinter Dahl and Kasper Tipsmark Therkildsen and not least research technician Frank Adrian for carrying out all the mechanical testing.

References

[1] Davis, J.R. ASM specialty handbook, "Tool Materials", ASM International, 1995

[2] C. Højerslev (2001). "Tool steels". Risø Report No. R-1244(EN), Risø National Laboratory, Roskilde, Denmark.

[3] C. Højerslev, J.V. Carstensen, P. Brøndsted, M.A.J. Somers (2002). "Fatigue Crack Behaviour in a High Strength Tool Steel". In: Proceedings of the 8th International Congress on Fatigue, EMAS, Stockholm.

[4] C. Højerslev, J.V. Carstensen, P. Brøndsted, M.A.J. Somers (2001). "Residual stresses in a M3:2 PM high speed steel; effect of mechanical loading". In: Proceedings of the 7th International Conference on Advanced Materials and Processes, EUROMAT, Rimini.

[5] Pedersen, Thomas Ørts. "Cyclic Plasticity and Low Cycle Fatigue in Tool Materials". Ph.D. Thesis. Institute for Solid Mechanics. The Technical University of Denmark. DCAMM report no. 582. 1998.

[6] Grønbæk, Jens. "The Use of Cyclic Material Data for Dimensioning Stripwound Cold Forging Tools". In Materialers Egenskaber - Modellering, Måling, Anvendelse. ed. Povl Brøndsted. Dansk Metallurgisk Selskab, Vintermødet, Sorø, Januar 2000. ISBN 87-87535-29-7

[7] Skov-Hansen, Peder. "Brudmekanisk undersøgelse af værktøjsmaterialer". M.Sc. Afhandling. Institut for Produktion, Danmarks Tekniske Universitet, MM-rapport nr. 96, 1996

[8] Brøndsted, P., Peder Skov-Hansen. "Fatigue Properties of High Strength Materials used in Cold-Forging Tools". Int. Journal of Fatigue. 20 (5), 1998, pp. 373-381

[9] Skov-Hansen, Peder, Niels Bay, Jens Grønbæk, Povl Brøndsted. "Fatigue in Cold-Forging Dies: Tool Life Analysis". Materials Processing Technology, 95, 1999, pp. 40-48

[10] Brøndsted, Povl. "Analytiske materialemodeller". I Plademateriale – Formgivning, Struktur og Egenskaber. Red. Povl Brøndsted, Kirsten Grønning Sørensen. Dansk Metallurgisk Selskab, Vintermødet, Grenå, Januar 1997. ISBN 87-87535-26-2

[11] Roberts, G.; Krauss, G.; Kennedy, R., "Tool Steels", 5th. Edition, ASM International, 1998

[12] Kristian Vinter Dahl. "Fractography analysis of tool samples used for cold forging". Risø-R-1360. August 2002.

[13] Kasper Tipsmark Therkildsen and Kristian Vinter Dahl. "Analysis of carbides and inclusions in high speed tool steels". Risø-R-1360. August 2002.

[14] Povl Brøndsted. "Experimental Measurements Of The Cyclic Plasticity". In Materials For Cold Forging Tool. Risø-I-1775. October 2001

[15] Christian Højerslev. Ph.D. thesis, December 2002.